Double-resonant Raman scattering in single-wall carbon nanotubes

J Maultzsch, S Reich, and C Thomsen

Technische Universität Berlin, Institut für Festkörperphysik, Hardenbergstr. 36, 10623 Berlin, Germany

E-mail: janina@physik.tu-berlin.de

Abstract. We present a new interpretation of the first-order Raman spectra of single-wall carbon nanotubes and compare them with experimental results. We suggest that the high-energy mode at ≈ 1600 cm^{-1} results from double-resonant Raman scattering and thus corresponds to a phonon mode from inside the Brillouin zone. We calculated the Raman cross section for general chiral tubes and are able to reproduce the experimental high-energy spectra in frequency and shape very well. Our model naturally explains the splitting of the two strongest peaks with the frequency of the highest peak being above the graphite Γ-point frequency. It further predicts the Raman frequencies to be laser-energy dependent and consequently a difference between Stokes and anti-Stokes spectra. Excitation-energy dependent Raman measurements support our model as they yield an increase in the splitting of the Raman peaks with increasing laser energy.

1. Introduction

Resonant Raman scattering provides information on both vibrational and electronic properties of the investigated material. Usually, in first-order scattering the phonon frequencies at the Γ point are observed, since for visible light the quasi-momentum conservation restricts the phonon wave vector to $q \approx 0$. In contrast, in carbon nanotubes the first-order Raman spectrum (i.e., the frequency range corresponding to single-phonon frequencies) appears to be dominated by a higher-order process where defect-scattering softens the $q \approx 0$ rule. Since large phonon wave vectors are allowed, a defect-induced process can lead to double-resonant scattering with two real intermediate states and hence a strongly enhanced Raman signal. Such a double-resonant process has been established as the origin of the disorder-induced D mode at around 1300 cm^{-1} in the Raman spectra of both graphite and carbon nanotubes and of its unusual excitation-energy dependence [1, 2].

Here we propose that in carbon nanotubes also the high-energy modes at 1600 cm^{-1} result from a double-resonant Raman process and correspond to phonon modes from inside the Brillouin zone [3]. In contrast to the usual interpretation, which attributes them to first-order Γ-point phonon modes, our model naturally explains the peculiar multiple-peak structure as well as the splitting and amplitude ratio between the two strongest peaks. We obtain our results by including only fully symmetric phonon modes, consistent with polarization-dependent experiments [4, 5, 6]. Moreover, our model predicts the high-energy mode to be excitation-energy dependent and Stokes and anti-Stokes spectra to be different. These two characteristic features of double-resonant scattering have been observed experimentally [3, 7]. We present excitation-energy dependent Raman measurements which show an upshift of the upper peak and a downshift of the lower peaks with increasing excitation energy in good agreement with our predictions.

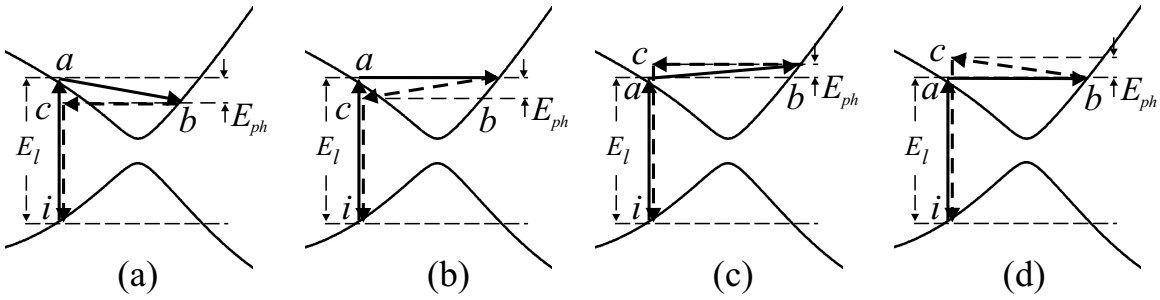

Figure 1. Defect-induced, double-resonant Raman processes with an incoming resonance. Solid and dashed arrows indicate resonant and non-resonant transitions, respectively. (a): an electron-hole pair is resonantly excited, the electron is resonantly scattered by emitting a phonon (Stokes), the electron is elastically scattered back by a defect, and the electron-hole pair recombines. (b): same as in (a), but the electron is first scattered elastically by a defect and then scattered back by a phonon; the involved phonon mode is different from the one in (a). (c) and (d): anti-Stokes scattering analogous to (a) and (b). Note that processes (b) and (d) lead to the same phonon mode. The corresponding processes with an outgoing resonance and those with scattering of the holes are not shown here.

2. Double-resonant Raman scattering

A defect-induced Raman process is a fourth-order process consisting of the excitation of an electron-hole pair, inelastic scattering of the electron (hole) by a phonon, elastic scattering of the electron (hole) by a defect and recombination of the electron-hole pair. The cross section for a given phonon mode with energy E_{ph} and wave vector q is proportional to [8]

$$|K_{2f,10}|^2 = \Big| \sum_{a,b,c} \frac{\mathscr{M}}{(E_l - E_{ai} - i\gamma)(E_l - E_{ph} - E_{bi} - i\gamma)(E_l - E_{ph} - E_{ci} - i\gamma)} + \frac{\mathscr{M}'}{(E_l - E_{ai} - i\gamma)(E_l - E_{bi} - i\gamma)(E_l - E_{ph} - E_{ci} - i\gamma)} \Big|^2,$$

where E_l is the laser energy, a, b, c denote the intermediate electronic states and i and f the initial and final states, respectively. We assume the matrix elements $\mathscr{M}$ and $\mathscr{M}'$ to be constant but include the selection rules for optical absorption and electron-phonon coupling [9, 10]; γ is the reciprocal lifetime of the intermediate states. The two terms in the sum refer to the different time order of phonon and defect scattering. The Raman process is called double-resonant, if two of the intermediate electronic states are real and thus two terms in the denominator vanish simultaneously. This causes a strong enhancement of the Raman cross section. A double-resonance condition can be fulfilled at any laser energy above the fundamental gap, since the elastic scattering by the defect allows conservation of wave vector for all phonon modes throughout the Brillouin zone.

In Fig. 1 (a) we show schematically a double-resonant process for Stokes scattering. An electron is resonantly excited by the incoming light and resonantly scattered by a phonon. The electron is elastically scattered back in a non-resonant transition and recombines with the hole. A unique combination of phonon wave vector q and energy E_{ph} satisfies the double-resonance condition for the particular excitation energy in the process shown in Fig. 1 (a). This phonon mode will be strongly enhanced compared with phonon modes which do not fulfill the double-resonance condition, and thus appear as a peak in the Raman spectrum. If the time ordering of the phonon and defect scattering is interchanged (Fig. 1 (b)), the enhanced phonon mode is slightly different from the one in Fig. 1 (a). Analogously, the double-resonant phonon mode is different for processes with an outgoing resonance (not shown here). In addition,

the asymmetry of the electronic bands around the extrema leads to slightly different Raman peaks for scattering from either side of the extrema. Thus a Raman peak resulting from a double-resonant process is never a single Lorentzian but rather consists of several close-by lines.

As a signature of double-resonant Raman scattering, the frequency of the Raman peaks depends on laser energy. For example, in Fig. 1 (a) the wave vector of the resonantly excited electron shifts away from the conduction band minimum for higher laser energy. Then a phonon mode with larger wave vector q and correspondingly different frequency $\omega_{ph}(q)$ becomes enhanced in the double-resonance process. Whether the dependence of the Raman frequencies on excitation energy can be observed experimentally, is determined by both the electronic structure and the phonon dispersion. A steep phonon dispersion leads to a large shift of the Raman frequencies as a function of laser energy. On the other hand, if the slope of the electron bands is large, the double-resonant phonon wave vector changes only slightly with laser wavelength.

Another characteristic of double-resonant scattering is the difference between Stokes and anti-Stokes spectra. In contrast to usual first-order Raman scattering, the Raman frequencies in Stokes and anti-Stokes scattering are different for a given laser energy. This can be easily understood from Fig. 1 (c). At the same laser energy the double-resonant phonon wave vector is in anti-Stokes scattering (with an incoming resonance and the phonon scattering first) significantly larger than in Stokes scattering (Fig. 1 (a)). Although processes (b) and (d) lead to the same phonon mode, the full Raman signal (including the corresponding processes with outgoing resonance) in anti-Stokes scattering is different from the Stokes signal; it can be easily seen that the anti-Stokes spectrum at a given laser energy corresponds to the Stokes spectrum taken at a higher laser energy.

Finally, the intensity of the Raman signal depends on excitation energy, similar to single-resonant scattering. If the incoming or outgoing resonance occurs close to the band extrema (high density of electronic states), the Raman intensity is larger than for transitions away from the band extrema. In addition, the Raman signal depends on the density of states of the involved phonon modes.

In summary, Raman spectra which result from double-resonant Raman scattering as in carbon nanotubes are determined by both the electron bands and the phonon dispersion relations throughout the Brillouin zone. In our calculations we use the electron bands found from zonefolding of the tight-binding results for graphene including third-nearest neighbors. This was shown to yield much better agreement with *ab initio* results than the first-neighbor tight-binding approximation [11]. For chiral tubes, we transformed the bands, which are given by the linear momentum k and quasi-angular momentum number m (defining the wave vector along the circumference), into the description by the fully conserved helical quantum numbers $\tilde{k}$ and $\tilde{m}$ [12]. The phonon dispersion relations are calculated from a symmetry-based force-constants approach described in Ref. [13]. From polarization-dependent measurements it is known that mainly fully symmetric phonon modes ($A_{1(g)}$ symmetry at the Γ point, where the subscript g refers to achiral tubes) contribute to the Raman signal [4, 5, 6]. Therefore we use in our calculations of the first-order spectra light polarized parallel to the tube axis (z) and the phonon bands with quasi-angular momentum number $\tilde{m} = 0$ ($A_{1(g)}$ symmetry). These phonon modes cannot change the band index $\tilde{m}$ of the electronic states, i.e., in first-order scattering the electrons are scattered always within the same band.

3. D and D^* mode

The D mode (at around 1300 cm^{-1}) in graphite and carbon nanotubes originates from a defect-induced, double resonant Raman process as described above [1, 2]. The involved

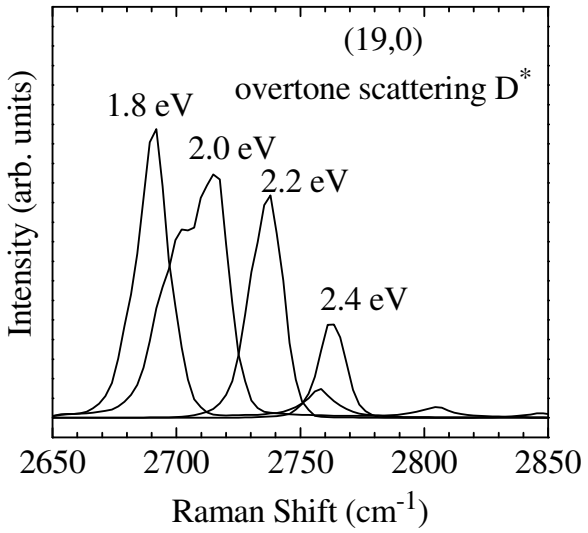

Figure 2. Calculated Raman spectrum of the D^* mode in the (19,0) tube with the reciprocal lifetime $\gamma = 0.03$ eV. The laser energy is given next to the peaks. The peak frequencies shift by about 120 cm^{-1}/eV.

phonon modes correspond to phonon modes around the K point in the graphite Brillouin zone. The frequency of the D mode shifts by about 50 cm^{-1}/eV with increasing excitation energy; because of non-linear electron and phonon dispersion relations and bundle effects the shift in carbon nanotubes is not simply linear [14].

From selection rules it was predicted that only tubes with $\mathscr{R} = 3$ exhibit the D mode systematically with its characteristic excitation-energy dependence [2, 15]. In tubes with $\mathscr{R} = 1$, phonon modes with frequencies close to the D-mode frequency exist at the Γ point, these are, however, forbidden by selection rules. Their band index m is large (e.g., $\approx 2n/3$ in zig-zag tubes); scattering of the electron by such a phonon changes the electron band index by m. This is incompatible with the optical transitions in the Raman process, which require $\Delta m = 0$ for z-polarized light.

In second order scattering, on the other hand, a second phonon with band index $m' = -m$ and wave vector $q' \approx -q$ can scatter the electron back to the original band [16]. Thus the second-order overtone D^* of the D mode will be observed in any tube. We consider, for instance, the zig-zag (19,0) tube ($\mathscr{R} = 1$), which does not exhibit the first-order D mode, and absorption of light into the electronic band $m_a = 14$. The excited electron can be scattered by a phonon $m_{ph} = 11$ (with a Γ-point frequency around the D-mode frequency) across the Γ point into the band $m_b = (m_a + m_{ph}) \bmod 2n = 25 - 38 = -13$. A second phonon with (nearly) the same frequency and $m_{ph} = -11$ scatters the electron back to the original band: $m_c = (-13 - 11) \bmod 38 = 14 = m_a$. In addition, we took the parities with respect to the horizontal mirror plane of the electron and phonon states into account.

In Fig. 2 we show the calculated second-order Raman spectra of the (19,0) tube for different laser energies. We find the D^* mode in the expected frequency range being clearly excitation-energy dependent. The energy shift of ≈ 120 cm^{-1}/eV is in reasonable agreement with experimental values [14, 17].

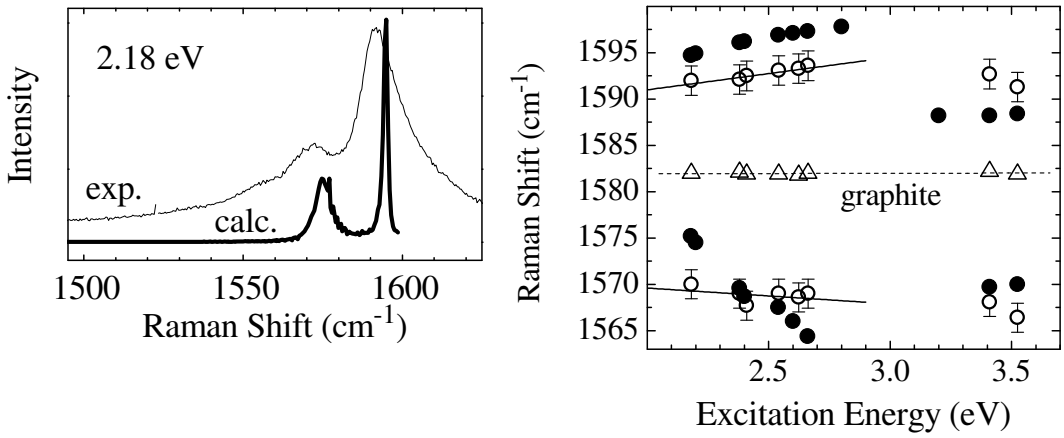

Figure 3. Left: Calculated high-energy spectrum of the (15,6) tube (thick line) and experimental spectrum of tube with a mean diameter of 1.45 nm (thin line) at $E_l = 2.18$ eV. The reciprocal lifetime $\gamma = 0.1$ eV. Right: Excitation-energy dependence of the high-energy mode of carbon nanotubes. The open and closed symbols denote experimental and calculated values, respectively. For comparison, the frequencies of the *G* mode in graphite are shown by open triangles. From Ref. [3].

4. High-energy mode

The defect-induced double-resonant Raman process in carbon nanotubes which leads to the *D* mode involves large phonon wave vectors and scattering across the Γ point. Consequently, other double-resonant processes are likely to occur. Instead of being scattered by phonons with relatively large wave vector, the resonantly excited electron can be scattered by phonons with small wave vectors across the conduction-band minimum. These phonon modes are (compared with the *D*-mode phonons) near-Γ-point modes and lead to Raman peaks with frequencies close to the Γ-point frequencies of the $\tilde{m} = 0$ phonon branches. We suggest that this process is the origin of the high-energy mode in the Raman spectra of carbon nanotubes [3].

In Fig. 3 (left) we show the calculated Raman spectrum of the (15,6) tube (thick line) and an experimental spectrum of bundled single-wall carbon nanotubes with a mean tube diameter of 1.45 nm (thin line) at an excitation energy of 2.18 eV. We find an excellent agreement between the calculated and the experimental spectrum with two main peaks at ≈ 1575 cm^{-1} and ≈ 1595 cm^{-1}. The highest peak corresponds to phonon modes near the overbending in the upper $\tilde{m} = 0$ phonon branch; the lower peaks originate from the second optical $\tilde{m} = 0$ phonon branch. Since the phonon density of states is particularly large close to the overbending, the amplitude of the peak at ≈ 1595 cm^{-1} is larger than of the other peaks. With increasing laser energy, the double-resonant phonon wave vector becomes larger (see Fig. 1). Therefore, the upper peak is expected to shift towards higher frequencies resembling the overbending, whereas the lower peaks shift in the opposite direction. In Fig. 3 (right) we show the Raman frequencies measured as a function of laser energy (open symbols). Indeed, we find that the splitting between the two main peaks increases with increasing excitation energy, as predicted by our model. For comparison the Raman frequencies of the *G* mode of graphite are shown (open triangles).

As long as for each laser energy the scattering process occurs in the same electronic band, the phonon wave vector and hence the splitting between the peaks continuously increases with increasing laser energy. If the excitation energy reaches the next higher electronic band,

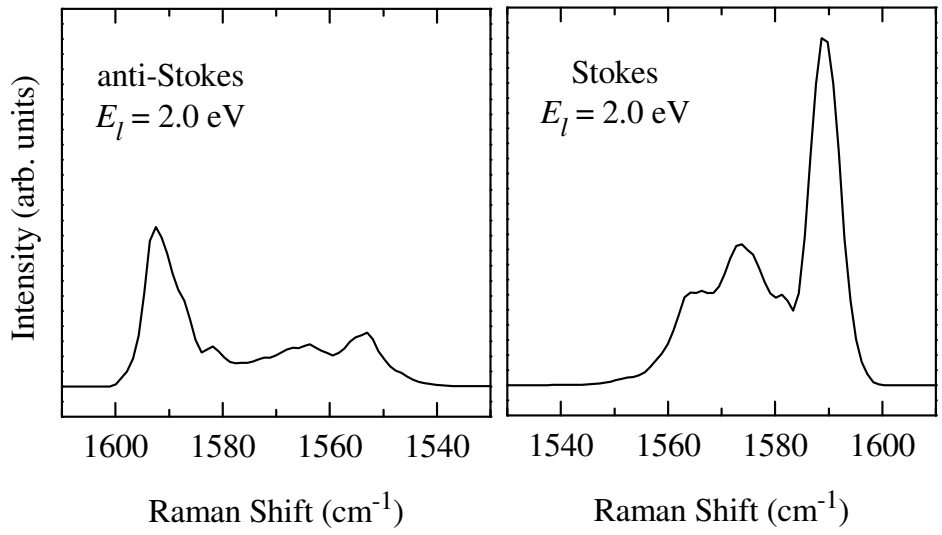

Figure 4. Anti-Stokes (left) and Stokes (right) spectrum of the high-energy mode of the (16,4) tube with an excitation energy of 2.0 eV and $\gamma = 0.1$ eV. The difference between anti-Stokes and Stokes spectra at the same laser energy arises from the different double-resonance conditions, see Fig. 1.

however, the double-resonant phonon wave vectors are again close to the Γ point. Scattering in this higher band dominates the spectra because of the high electronic density of states near the band extrema. Therefore, the splitting between the Raman peaks becomes abruptly smaller and then increases again with further increasing laser energy. This can be seen in Fig. 3 for $E_l > 3$ eV.

As described above, another consequence of the double-resonance model is the difference between Stokes and anti-Stokes spectra at a given excitation energy. In Fig. 4 we show the anti-Stokes (left) and Stokes spectrum (right) calculated for the (16,4) tube at a laser energy of 2.0 eV. They differ in both frequency and shape (relative peak intensities) as observed experimentally, see for instance Ref. [7]. We find from excitation-energy dependent calculations that the anti-Stokes spectrum at a given laser energy E_l is roughly the same as the Stokes spectrum at $E_l + E_{ph}$. It can be seen from Fig. 1 (and the corresponding scattering processes with an outgoing resonance) that this holds in general for double-resonant scattering.

In summary, our model of double-resonant Raman scattering as the origin of the high-energy mode in carbon nanotubes is supported by several experimental findings. These are the peak structure of the high-energy mode with all peaks arising from fully symmetric phonon modes, the splitting and amplitude ratio of the two main peaks, the excitation-energy dependence of the Raman frequencies and the difference in Stokes and anti-Stokes scattering.

5. Conclusion

We showed that besides the defect-induced D mode and its overtone D^* the high-energy mode in the first-order Raman spectra of single-wall carbon nanotubes results from double-resonant Raman scattering. This interpretation naturally explains the observed symmetry, frequencies and peak shape of the high-energy mode. Our model predicts an excitation-energy dependence of the Raman frequencies and a difference between Stokes and anti-Stokes scattering, which is both in very good agreement with experiments.

Consequently, we predict the radial breathing mode (RBM) to originate from double-resonant scattering as well. In contrast to the *D* mode and the high-energy mode, we expect no significant excitation-energy dependence because of the nearly flat phonon dispersion of the RBM close to the Γ point.

We thank E. Dobardžić, I. Milošević, and M. Damnjanović for providing us with the phonon dispersion relations. This work was supported by the Deutsche Forschungsgemeinschaft under Grant No. Th 662/8-1.

References

[1] Thomsen C and Reich S 2000 Phys. Rev. Lett. 85 5214
[2] Maultzsch J, Reich S and Thomsen C 2001 Phys. Rev. B. 64 121407(R)
[3] Maultzsch J, Reich S and Thomsen C 2002 Phys. Rev. B. 65 233402
[4] Duesberg G S, Loa I, Burghard M, Syassen K and Roth S 2000 Phys. Rev. Lett. 85 5436
[5] Jorio A, Dresselhaus G, Dresselhaus M S *et al.* 2000 Phys. Rev. Lett. 85 2617
[6] Reich S, Thomsen C, Duesberg G S and Roth S 2001 Phys. Rev. B 63 041401(R)
[7] Brown S D M, Corio P, Marucci A, Dresselhaus M S, Pimenta M A and Kneipp K 2000 Phys. Rev. B 61 R5137
[8] Martin R M and Falicov L M 1983 in Light Scattering in Solids I edited by Cardona M, Topics in Applied Physics Vol. 8 (Berlin: Springer) p 79
[9] Damnjanović M, Milošević I, Vuković T, and Sredanović R 1999 Phys. Rev. B 60 2728
[10] Božović I, Božović N and Damnjanović M 2000 Phys. Rev. B 62 6971
[11] Reich S, Maultzsch J, Thomsen C and Ordejón P 2002 Phys. Rev. B in print
[12] Damnjanović M, Vuković T and Milošević I 2000 J. Phys. A: Math. Gen. 33 6561
[13] Maultzsch J, Reich S, Thomsen C, Dobardžić E, Milošević I and Damnjanović M 2002 Solid State Comm. 121 471
[14] Kürti J, Zólyomi V, Grüneis A and Kuzmany H 2002 Phys. Rev. B 65 165433
[15] $\mathscr{R} = 3$ if $(n_1 - n_2)/3n$ is integer and $\mathscr{R} = 1$ else, following the notation used in Ref. [9]. n_1 and n_2 are the components of the chiral vector in the basis of the graphene lattice vectors; n denotes the greatest common divisor of (n_1, n_2).
[16] This is in contrast to defect scattering, where the defect cannot change the quasi-angular momentum quantum number m of the electronic state.
[17] Thomsen C 2000 Phys. Rev. B 61 4542